An Extension of the Swarmalator Model

Ankith Anil Das
470485327
Faculty of Science, Mathematics
The University of Sydney
Email: aani9804@uni.sydney.edu.au

Synchronization occurs at many natural and technological systems. Such an emergent properties is observed in cardiac pacemaker cells, Japanese tree frogs, colloidal suspensions of magnetic particles, and other biological and technological systems in which synchronization interact. We consider the system where oscillators can sync and swarm. A detailed analysis was proposed by Kevin P. O'Keeffe in the paper "Oscillators the sync and swarm". We studied an extended model of the Swarmalator model proposed in the paper. Understanding the dynamics of this model could possibly give insight to the generalized model where the phase coupling function could be a fourier series.

1 Introduction

2 The Model

We consider swarmalators free to move in the plane. The governing equations are

$$\dot{\mathbf{x}}_i = \mathbf{v}_i + \frac{1}{N}\sum_{j=1}^{N}\left[\mathbf{I}_{\text{att}}\left(\mathbf{x}_j-\mathbf{x}_i\right)F\left(\theta_j-\theta_i\right)-\mathbf{I}_{\text{rep}}\left(\mathbf{x}_j-\mathbf{x}_i\right)\right] \tag{1}$$

$$\dot{\theta}_i = \omega_i + \frac{K}{N}\sum_{j=1}^{N} H_{\text{att}}\left(\theta_j-\theta_i\right)G\left(\mathbf{x}_j-\mathbf{x}_i\right) \tag{2}$$

for $i = 1,\ldots,N$, where N is the number of swarmalators, $\mathbf{x}_i$ is the position of the i-th swarmalator, and θ_i, ω_i, and $\mathbf{v}_i$ are it's phase, natural frequency and background velocity. The functions $\mathbf{I}_{att}$ and $\mathbf{I}_{rep}$ represent spatial attraction and repulsion between the swarmalators where as phase interaction is governed by $\mathbf{H}_{att}$. We considered the following model:

$$\dot{\mathbf{x}}_i = \mathbf{v}_i + \frac{1}{N}\left[\sum_{j\neq i}^{N}\frac{\mathbf{x}_j-\mathbf{x}_i}{\left|\mathbf{x}_j-\mathbf{x}_i\right|}\left(1+J\cos\left(\theta_j-\theta_i\right)\right)-\frac{\mathbf{x}_j-\mathbf{x}_i}{\left|\mathbf{x}_j-\mathbf{x}_i\right|^2}\right] \tag{3}$$

$$\dot{\theta}_i = \omega_i + \frac{K}{N}\sum_{j\neq i}^{N}\frac{\gamma_1\sin\left(\theta_j-\theta_i\right)+\gamma_2\sin\left(2\left(\theta_j-\theta_i\right)\right)}{\left|\mathbf{x}_j-\mathbf{x}_i\right|} \tag{4}$$

We considered identical swarmalators so that $\omega_i = \omega$ and $\mathbf{v}_i = \mathbf{v}$. Using this assumption, using a suitable choice of reference frame we can set $\omega = 0$, and $\mathbf{v} = \mathbf{0}$. The system has four parameters $(J, K, \gamma_1, \gamma_2)$.

The parameter J measures the extend to which phase similarity enhances spatial attraction. For $J > 0$, swarmalators prefer to be near other swarmalators with similar phase. When $J < 0$, the opposite behavior is observed: swarmalators attract those with opposite phase. When $J = 0$, they show no phase based spatial behavior,i.e, their spatial attraction is independent of phase. To maintain $\mathbf{I}_{att} > 0$, we constrain J to $-1 \leq J \leq 1$. The parameter K is the phase coupling strength which scales γ_1, and γ_2. The relative strengths of γ_1 and γ_2 determine the stability of one or two clusters.

Before stating the dynamics of the system, we pause to state the features of this model. This model's purpose is to study the interplay between swarming and synchronization. Our model accounts for aggregation, but not alignment. There are no alignment terms. We chose to neglect orientation because it adds another layer of complexity; it makes each swarmalator have four state variables. For rest of the report we will refer to our model as 'Dual phase coupled model' because of the presence of double angle sin function in Eq.4. In a similar fashion, the original model proposed by Kevin P. O'Keeffe will be referred as 'Single phase coupled model'.

3 Optimization of the ode solver

The simulations were run using MATLAB's ODE integrator 'ode45'. Absolute and Relative tolerance for the integrator was set to 10^{-6}. Before large computations were performed, optimisation of the existing code was necessary. As this project involves computations of large matrices using ode45, optimising the code for speed was essential for any extensive calculation. The initial code was profiled using

MATLAB's performance profiler, and bottlenecks were identified. Calculating the pairwise inverse distance was the most computationally expensive part in the ode function. The original code took 70 seconds for a simulation with $N = 100$ and $T = 10$-time units. This speed was too slow for any extended time simulations. After removing unwanted function calls, changing the algorithm, and using functions which supports vectorization, the new code took 0.509 sec for the same task. The performance was good enough for an interactive user simulation where the user can change the parameters of the system and can see the results almost instantly.

4 Cluster formation and stability

The dynamics of dual phase coupled model had some striking differences with the original single phase model. The system not only settled in all the five states which were discussed in detail by Kevin P. O'Keeffe in single phase model, but also showed many additional stable and metastable states. Understanding the behavior of the modified phase coupling term and how it affects the formation of states could give us deep insights about the generalization of the model. The additional cluster states made by the model can be broadly classified as follows

(a) Static two cluster state
(b) Static bimodal single cluster state.
(c) Two cluster state with rogues
(d) Active 4 cluster state
(e) Active single cluster state

To understand system behavior under the change of γ_1, and γ_2, we chose $J = 0.8$ and $K = -0.5$ which represent Active phase wave in single phase coupled model. This set of state variables were chosen because it showed the most active spacial behavior in single phase coupled model and the dynamics of the system would be more depended on the values of γ_1 and γ_2. Unless otherwise stated, the simulations are run with $J = 0.8$ and $K = -0.5$. Also, all the simulations were run with random initial position in a 1x1 box and phases from $[-\pi, \pi]$, both uniformly and random. To maintain consistency, the same random seed was used for all simulations.

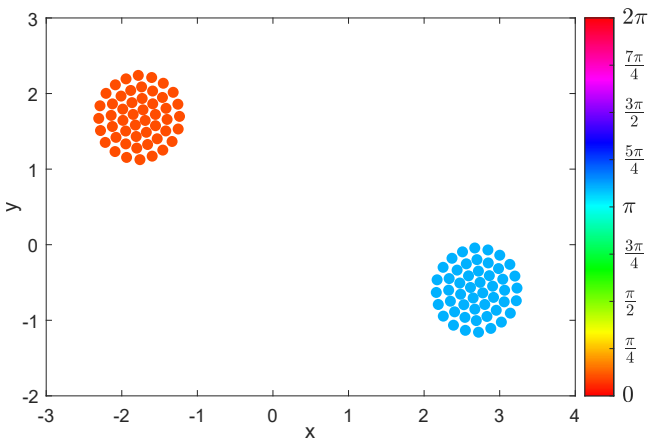

Fig. 1. Static two Cluster State. This state was achieved for $N = 100$, $\gamma_1 = 1/3$, and $\gamma_2 = -0.5$. The simulation was run for $T = 100$ time steps with variable step-size (ode45) for the system to settle down.

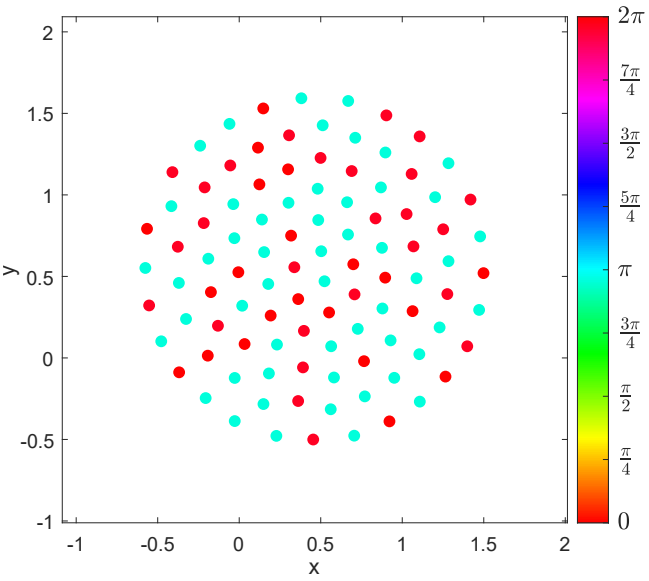

Fig. 2. Static bimodal single cluster state.

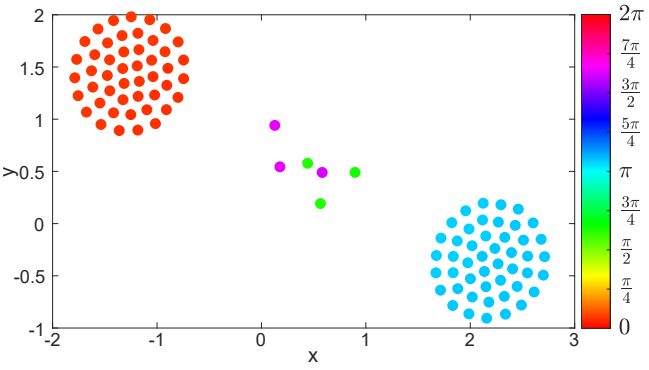

Fig. 3. Two Clusters with Rogues

4.1 Static Two cluster state

Static two cluster case is a very common equilibrium state seen for various values of $(J, K, \gamma_1, \gamma_2)$, illustrated in Fig.1. Since $J > 0$, 'like attracts like': swarmalators want to settle near other swarmalators with similar phase. Looking at phase dynamics equation (Eq.4) $\dot{\theta}_i = 0$ when $\theta_i = C, C + \pi$, where C is any constant. Due to the presence of a new stable phase, the system can form two clusters with π phase difference. Now for the given value of K which is less than 0, $\gamma_1 > 0$ (Some coupling) implies the system does not prefer single cluster state, and $\gamma_2 < 0$ (other coupling) means the system prefers to stabilize in two cluster state. Furthermore, $|\gamma_2| > |\gamma_1|$ shows that the second coupling term in Eq.4 is more dominant in stabilizing the system. Fig.6 shows how the phase settles with time. Here, the phase effectively stabilizes to two values after taking mod 2π. The average cluster phase difference is approximately π with an absolute error $\varepsilon \approx 2.6074 \times 10^{-9}$. Our statement about two cluster phase difference therefore agrees with the simulations.

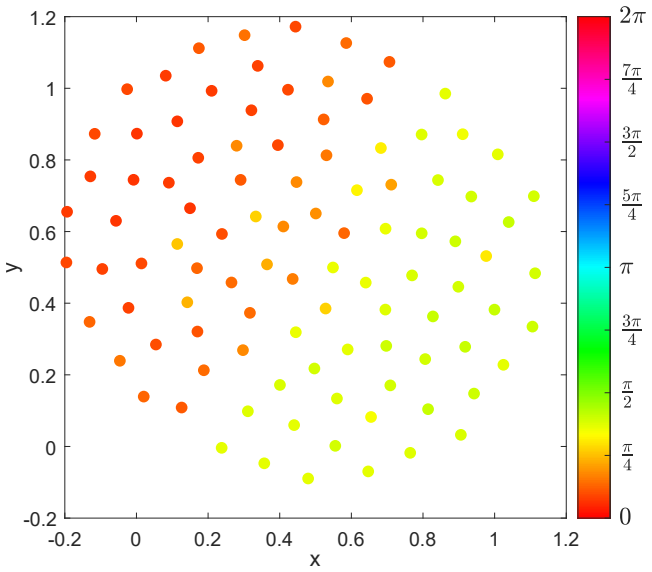

Fig. 4. Active Single cluster state

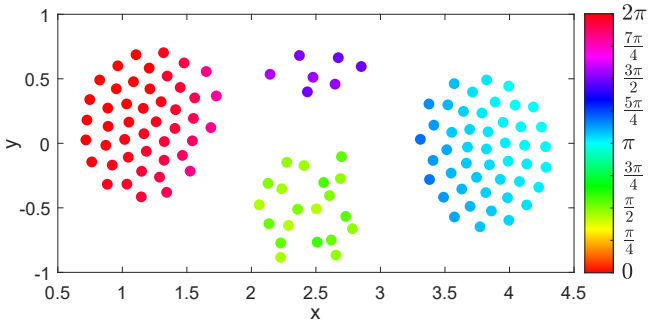

Fig. 5. Active 4 cluster state

4.2 Inter-cluster distance for Static two cluster state

We can analytically solve the inter-cluster distance for static two cluster state by making an assumption. Let,

$$\mathbf{C}_0 = \frac{1}{N_0}\sum_{i\in S_0}\mathbf{x}_i \qquad \text{and} \qquad \mathbf{C}_\pi = \frac{1}{N_\pi}\sum_{i\in S_\pi}\mathbf{x}_i, \tag{5}$$

where $\mathbf{C}_0$ and $\mathbf{C}_\pi$ are the centroids of the clusters with average phase approximately equal to 0 and π respectively , and S_0 and S_π are the respective clusters. Differentiating $\mathbf{C}_0$ w.r.t time gives

$$N_0\dot{\mathbf{C}}_0 = \sum_{i\in S_0}\dot{\mathbf{x}}_i = \sum_{i\in S_0}\left(\sum_{j=1}^{N}\frac{\mathbf{x}_j-\mathbf{x}_i}{|\mathbf{x}_j-\mathbf{x}_i|}(1+J\cos(\theta_j-\theta_i)) - \frac{\mathbf{x}_j-\mathbf{x}_i}{|\mathbf{x}_j-\mathbf{x}_i|^2}\right)$$

$$= \sum_{i\in S_0}\left(\underbrace{\sum_{j\in S_0}\left(\frac{\mathbf{x}_j-\mathbf{x}_i}{|\mathbf{x}_j-\mathbf{x}_i|}(1+J) - \frac{\mathbf{x}_j-\mathbf{x}_i}{|\mathbf{x}_j-\mathbf{x}_i|^2}\right)}_{=0,\text{since pair wise cancellation}} + \sum_{j\in S_\pi}\left(\frac{\mathbf{x}_j-\mathbf{x}_i}{|\mathbf{x}_j-\mathbf{x}_i|}(1+J) - \frac{\mathbf{x}_j-\mathbf{x}_i}{|\mathbf{x}_j-\mathbf{x}_i|^2}\right)\right)$$

$$= \sum_{i\in S_0}\sum_{j\in S_\pi}\frac{\mathbf{x}_j-\mathbf{x}_i}{|\mathbf{x}_j-\mathbf{x}_i|^2}((1+J)|\mathbf{x}_j-\mathbf{x}_i|-1)$$

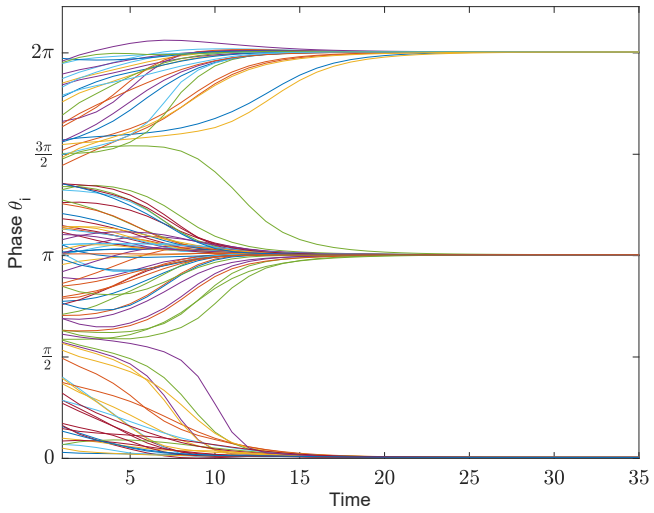

Fig. 6. Phase of the Swarmalator vs Time.

We will make the assumption that $|\mathbf{x}_j-\mathbf{x}_i| \approx |\mathbf{C}_0-\mathbf{C}_\pi| = r$ (say). Then

$$N_0\dot{\mathbf{C}}_0 \approx \sum_{i\in S_0}\sum_{j\in S_\pi}\frac{\mathbf{x}_j-\mathbf{x}_i}{r^2}((1+J)r-1)$$

$$= \frac{(1+J)r-1}{r^2}\left(\sum_{i\in S_0}\sum_{j\in S_\pi}\mathbf{x}_j-\mathbf{x}_i\right)$$

$$\dot{\mathbf{C}}_0 = N_\pi\frac{(1+J)r-1}{r^2}(\mathbf{C}_\pi-\mathbf{C}_0). \tag{6}$$

Using similar arguments we can also find $\dot{\mathbf{C}}_\pi$,

$$\dot{\mathbf{C}}_\pi = N_0\frac{(1+J)r-1}{r^2}(\mathbf{C}_0-\mathbf{C}_\pi). \tag{7}$$

Finally,

$$\dot{\mathbf{C}}_0-\dot{\mathbf{C}}_\pi = -N\left(\frac{(1-J)r-1}{r^2}\right)(\mathbf{C}_0-\mathbf{C}_\pi)$$

$$\Rightarrow \frac{dr}{dt} = -N\left(\frac{(1-J)r-1}{r}\right). \tag{8}$$

Equating Eq.8 to zero gives the equilibrium distance between the cluster,

$$r^* = \frac{1}{1-J} \tag{9}$$

Surprisingly but yet obvious, the inter-cluster distance is independent of N, K, γ_1 and γ_2. To verify our analytical solution, simulations were run for various values of N and K and the results are shown in Fig.7 and Fig.8. These figures shows agreement between these predictions and simulations. Also, from Eq.9, we realize that for $J \geq 1$ the two clusters move to infinity.

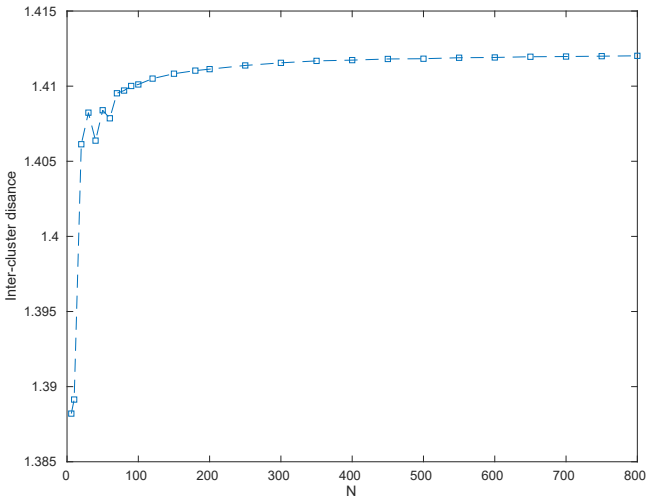

Fig. 7. Inter-cluster distance for static two cluster state. Simulations were run for various values of N with $K = -0.5, J = 0.3, \gamma_1 = 2/3, \gamma_1 = -1/3$. Swarmalators were initially positioned in two equally sized clusters with average phase 0 and π and simulations were run for $T = 300$ time steps.

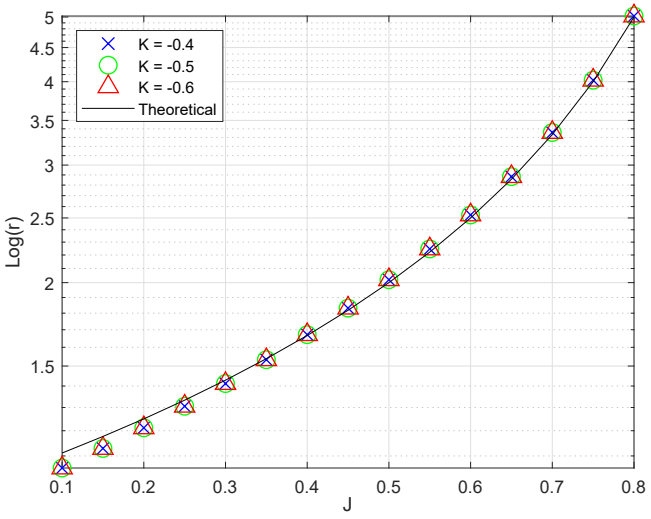

Fig. 8. Inter-cluster distance for varying K. Simulations were run for various values of K and J for $N = 800$. The black line shows the theoretical prediction as per Eq.9. The figure justifies that inter-cluster distance is independent of K.

5 Two clusters with Rogues

5.1 Stability of Static two cluster state

6 Periodic motion of Rogues

7 Circular ring state

In a search for more stable states, we encountered a special unstable equilibrium state which could be achieved by careful arrangement of swarmalators. It is achieved by placing swarmalators around a circle of half unit radius with a single swarmalator in the center. The circumferential and central swarmalators have a phase difference of π. The arrangement of swarmalators is shown in Fig. 9. Initially, the system collapses to a stable radius and maintains approximately the same radius for some time. After a critical time, the system destabilizes into two clusters. This result is shown in Fig. 10. We also looked at the distance between the centroid of the circumferential swarmalators and the center swarmalator. From Fig. 11, we realized that a small perturbation in the arrangement of swarmalators grows exponentially until the system destabilizes into two clusters. To check if this destabilization was due to the numerical solver, we changed the absolute and relative error tolerance to 10^{-10} and this resulted in a slight increase in stable time. Further decrease in error order did not increase the stable time of the system. We also ran the simulation in single precision mode by adding an error term of order 10^{-8} to the solver function. This change to single precision decreased the stable time by half as shown in Fig.12. These tests does not confirm the numerical instability of the ode solver, but it does give insight into the sensitivity of such configuration.

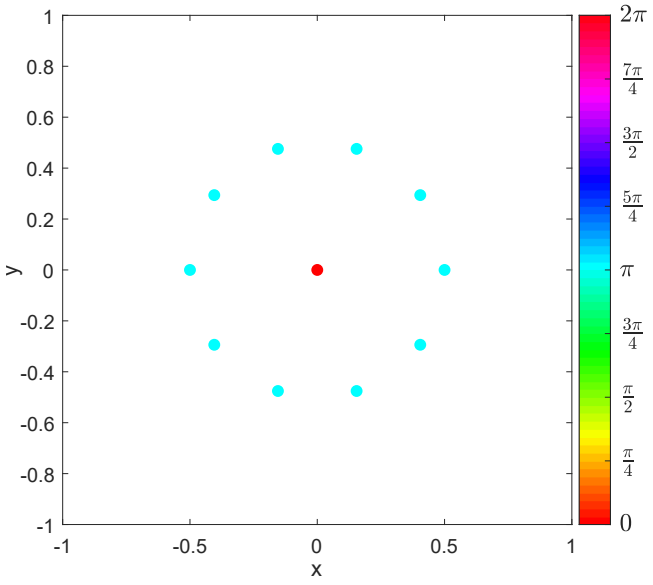

Fig. 9. Circular arrangement of swarmalators. Here the central swarmalator has phase 0 and the circumferential swarmalators have a phase π. The system has $N = 11$ swarmalators with $\gamma_1 = 2/3, \gamma_1 = -1/3$

8 Phase Variation within the clusters

So far, we have explored the collective behaviour of swarmalator in forming clusters. In this section, we will briefly talk about the behaviour of swarmalators within the cluster formation. For static two cluster case, there was little to no phase variation within the cluster. The calculated standard deviation of phase within the cluster was 2.678×10^{-17}, which for all numerical purpose is effectively zero. This is indeed quite surprising as we expected a phase gradient within the cluster due to the presence of the other cluster. Finally, adding random phase variations within the cluster led the cluster to stabilize to a different constant uniform value throughout the cluster. The average phase difference between the cluster was still approximately π.

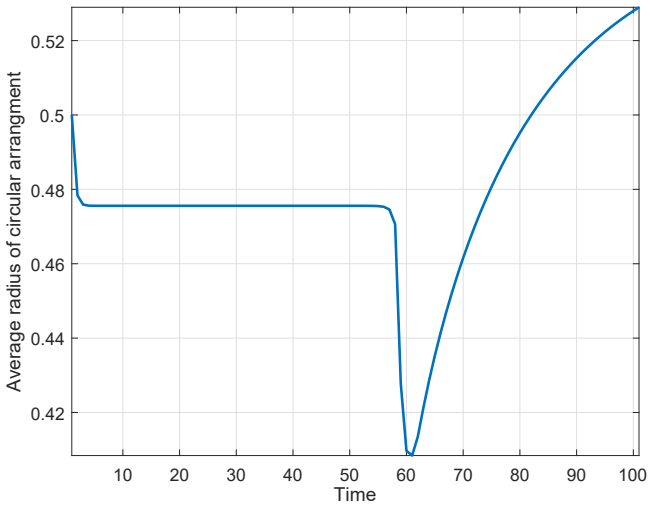

Fig. 10. Average distance of the swarmalators from the center. The circumferential swarmalators collapse to a stable radius until it destabilizes into two clusters.

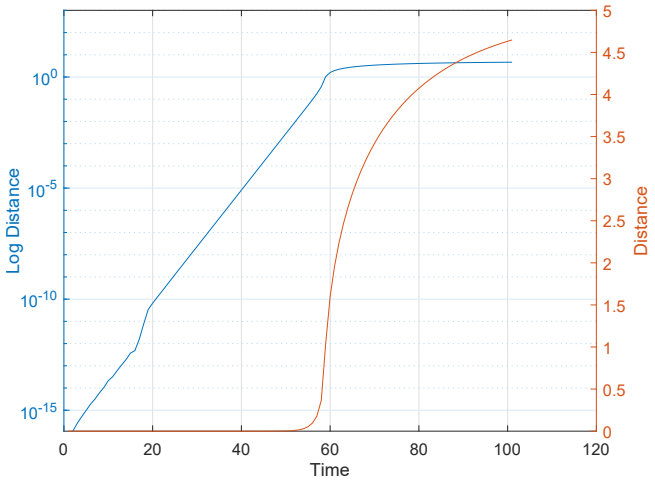

Fig. 11. Distance between the centroid of circumferential swarmalators and center swarmalator. We can see that a small perturbation of order 10^{-16} builds up exponentially until the system destabilizes into two clusters

Static bimodal single cluster is a special case where $J = 0$. The single cluster behaviour was expected as the system is effectively phase decoupled, i.e. Eq.3 has no phase term. This results in a single cluster lattice structure where the phase stabilizes to either 0 or π. Fig.2 shows the structure after the system settles.

Finally, we looked into two cluster state with rogues. To amplify the phase variations within the cluster, we ran the simulations for $N = 400$. After the system settled into two clusters with rogues in the middle, the clusters show oscillatory phase distribution within the cluster, as shown in Fig.13. There was a smooth gradient in phase, and the two clusters showed opposite phase distribution as the rogues moved back and forth.

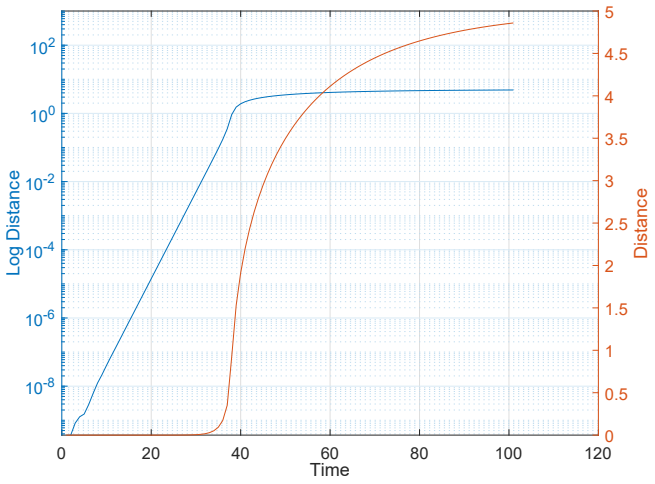

Fig. 12. Distance between the centroid of circumferential swarmalators and center swarmalator run at single precision mode. Single precision mode was simulated by adding random numbers of order 10^{-8} to the solver function. Comparing with Fig.11, the stable time has been almost reduced by half.

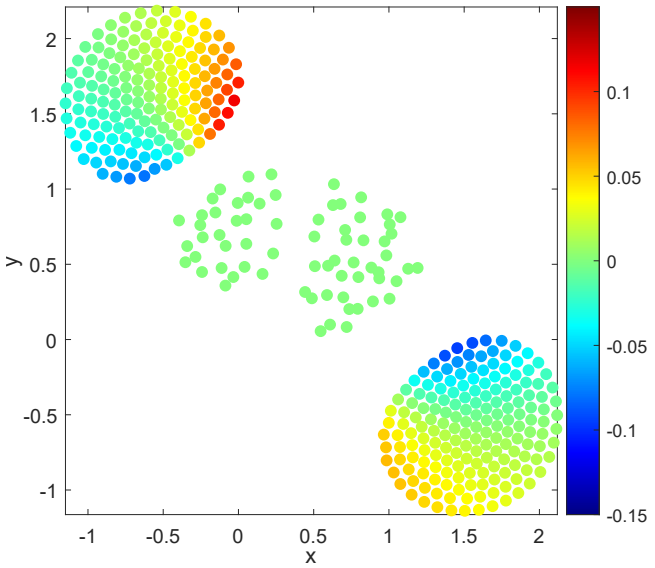

Fig. 13. Phase variation within the cluster. This simulation was run for $N = 400$ with $\gamma_1 = 2/3, \gamma_1 = -1/3$. The phase of each cluster was centered to zero by using the average phase of the cluster. The color gradient shows the variation of phase within the cluster. The phase of all rouges (center swarmalators) was set to zero for better visualization.

9 Simplified model
10 Front end application
11 Conclusion
12 References